

Fluorogenic Probes for Multicolor Imaging in Living Cells

Gražvydas Lukinavičius,^{*,†,§,#} Luc Reymond,^{*,†,§,#} Keitaro Umezawa,[‡] Olivier Sallin,[†] Elisa D'Este,[§] Fabian Göttfert,[§] Haisen Ta,[§] Stefan W. Hell,[§] Yasuteru Urano,[‡] and Kai Johnsson^{*,†}

[†]Institute of Bioengineering, NCCR in Chemical Biology, Institute of Chemical Sciences and Engineering (ISIC), Ecole Polytechnique Fédérale de Lausanne (EPFL), 1015 Lausanne, Switzerland

[‡]Graduate School of Pharmaceutical Sciences, The University of Tokyo, 7-3-1, Hongo, Bunkyo-ku, Tokyo 113-8654, Japan

[§]Department of NanoBiophotonics, Max-Planck-Institute for Biophysical Chemistry, Am Fassberg 11, 37077 Göttingen, Germany

Supporting Information

ABSTRACT: Here we present a far-red, silicon-rhodamine-based fluorophore (SiR700) for live-cell multicolor imaging. SiR700 has excitation and emission maxima at 690 and 715 nm, respectively. SiR700-based probes for F-actin, microtubules, lysosomes, and SNAP-tag are fluorogenic, cell-permeable, and compatible with super-resolution microscopy. In conjunction with probes based on the previously introduced carboxy-SiR650, SiR700-based probes permit multicolor live-cell superresolution microscopy in the far-red, thus significantly expanding our capacity for imaging living cells.

Fluorescence microscopy is a powerful approach for live-cell imaging. While important advances are continuously made to acquire and analyze data, the development of appropriate fluorescent probes lags behind.¹ A fluorescent probe suitable for applications inside living cells needs to be membrane permeable but must not display unspecific interactions with the sample. Furthermore, such a probe should be bright and photostable and, ideally, excitable at far-red or near-infrared wavelengths in order to decrease phototoxicity and background. Before now, only a small fraction of existing fluorophores fulfilled these conditions.² Among them, carboxylated silicon-rhodamines (carboxy-SiR, Figure 1A) appear particularly well suited for imaging living cells.^{3–8} Carboxy-SiRs display far-red emission and excitation wavelengths, are suitable for super-resolution microscopy and carboxy-SiR-based probes tend to be cell permeable and fluorogenic. The 2'-carboxyl group mediates the latter two properties: carboxy-SiRs show a much higher tendency than conventional rhodamines or carbopyronines to exist in their nonfluorescent spirocyclic form (Figure 1A). While this may look disadvantageous, it can render carboxy-SiR-based probes fluorogenic: we have previously shown that binding of carboxy-SiR-based probes to their respective targets shifts the equilibrium back toward the fluorescent zwitterion. This has allowed the generation of fluorogenic carboxy-SiR-based probes for live-cell imaging of self-labeling protein tags, cytoskeletal proteins, receptor proteins, unnatural amino acids, lipids as well as DNA.^{3–5,9–11} However, a carboxy-SiR derivative with further red-shifted excitation and emission wavelengths for multicolor live cell imaging is still lacking. Here we introduce SiR700, a new carboxy-SiR fluorophore, which in

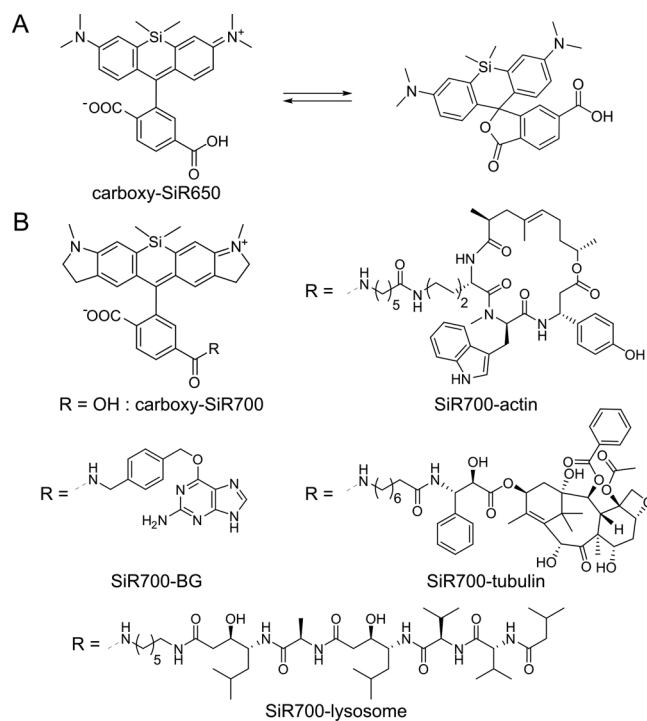


Figure 1. Carboxy-SiR-based probes. (A) Spirolactone–zwitterion equilibrium of carboxy-SiR650. (B) Chemical structures of carboxy-SiR700 based probes. The ligands used for the F-actin, microtubules, SNAP-tag, and lysosome probes were jasplakinolide, docetaxel, benzylguanane, and pepstatin A, respectively.

combination with carboxy-SiR650, permits live-cell dual-color superresolution microscopy in the far-red.

Our design of a carboxy-SiR derivative with further red-shifted excitation wavelength was based on previous work in which it was shown that introduction of an indoline into the SiR scaffold results in a 50 nm red-shift of its emission and excitation maxima.¹² However, this compound did not bear the 2'-carboxyl group that confers the fluorogenic properties. We therefore prepared and characterized carboxy-SiR700 (Figure 1B) via a route analogous to carboxy-SiR650³ (Supplementary Figure 1). The excitation and emission maxima of carboxy-

Received: May 9, 2016

Published: July 15, 2016

SiR700 were determined to be 687 and 716 nm, respectively. The emission is therefore approximately 50 nm red-shifted when compared to SiR650 (Figure 2A). Its extinction

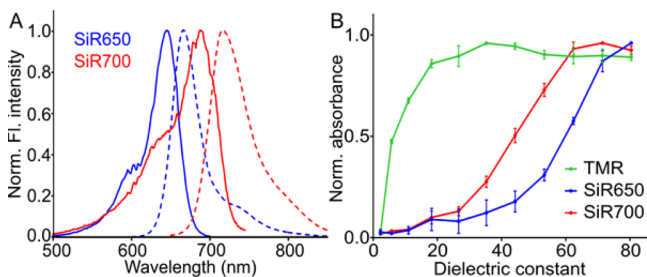


Figure 2. Properties of fluorophores. (A) Fluorescence excitation (solid lines) and emission (dashed lines) spectra of carboxy-SiR650 (blue) and carboxy-SiR700 (red). (B) Sensitivity of zwitterion-spirolactone equilibrium of TMR (green), carboxy-SiR650 (blue), and carboxy-SiR700 (red) to the dielectric constant of solvent.

coefficient (ϵ_{\max}) is $100\,000\text{ M}^{-1}\cdot\text{cm}^{-1}$, and its quantum yield (Φ_f) is 0.13 in water (Supplementary Table 1).¹² While these spectroscopic properties are nearly identical to the values reported for the SiR700 analogue having a 2'-methyl group,¹² the 2'-carboxy group permits the dye to form the non-fluorescent spirolactone. This is evident from water-dioxane titrations in which SiR700 transitions from a zwitterionic state to the dark spirolactone at decreasing dielectric constant, as measured by the decrease of absorbance between 500 and 750 nm (Figure 2B, Supplementary Figure 3C). The propensity of carboxy-SiR700 to form the spirolactone is slightly lower than carboxy-SiR650 but much higher than TMR: The D50 value, defined as the dielectric constant at which absorbance of fluorophore solution is decreased by half compared to the highest recorded absorbance, of carboxy-SiR700 was measured to be 43, whereas those of carboxy-SiR650 and TMR were measured to be 59 and 6.4, respectively. These data indicate that carboxy-SiR700 is a suitable starting point for the creation of fluorogenic and far-red probes. Therefore, we coupled carboxy-SiR700 to the following targeting ligands as previously applied for carboxy-SiR650: jasplakinolide for binding to F-actin (SiR700-actin); docetaxel for binding to microtubules (SiR700-tubulin); benzylguanidine for reacting with SNAP-tag (SiR700-BG) (Figure 1B).¹³ We also attempted to create new SiR-based probes for imaging lysosomes. Lysosomes are membrane-bound cell organelles dedicated to the degradation of biomolecules in an acidic environment of pH 4.5. Although they vary in shape and size, lysosomes can be approximated as spherical vesicles of 0.1–1 μm diameter. As targeting ligand we chose pepstatin A, which is a potent inhibitor of the lysosome-resident protease cathepsin D and which has previously been used for the design of fluorescent probes.¹⁴ Pepstatin A was coupled to both carboxy-SiR650 and carboxy-SiR700, yielding SiR-lysosome and SiR700-lysosome, respectively (Figure 1B, Supplementary Scheme 6).

We then characterized all new probes for target binding in vitro. SiR700-BG reacted with SNAP-tag with a second-order rate constant of $1.8 \times 10^4\text{ M}^{-1}\cdot\text{s}^{-1}$, which is close to the value of $3.5 \times 10^4\text{ M}^{-1}\cdot\text{s}^{-1}$ of the corresponding carboxy-SiR650 analogue SiR-SNAP (Supplementary Table 4). As judged by actin and tubulin polymerization assays, SiR700-actin and SiR700-tubulin were both found to interact with their respective targets to the same extent as the previously reported

carboxy-SiR650-based probes SiR-actin and SiR-tubulin. SiR-lysosome and SiR700-lysosome both inhibited pepsin efficiently (Supplementary Figure 2). We then investigated the fluorogenicity of the new probes by measuring the increase of fluorescence either upon interaction with their target or upon addition of the surfactant SDS (Supplementary Tables 2 and 3). The fluorescence increase upon target binding for the carboxy-SiR700-based probes ranked between 4- and 21-fold, depending on the ligand. The hydrophobicity (calculated LogD) of the probes strongly correlates with their fluorogenicity (Supplementary Figure 3, Supplementary Table 5). This supports our hypothesis that target binding shifts the equilibrium to the fluorescent zwitterion. The fluorogenicity observed for carboxy-SiR700-based probes is smaller than those observed for carboxy-SiR650-based probes but much higher than those observed for TMR-based probes, which is in agreement with the data from the water-dioxane titrations. To further investigate the mechanism of fluorogenicity of SiR-based probes, we measured the fluorescence lifetimes of carboxy-SiR700-, carboxy-SiR650-, and SiR-based probes (Supplementary Table 6). The measured lifetimes of carboxy-SiR650 and carboxy-SiR700 of 2.7 and 1.4 ns increased by up to 1.1 ns after their conjugation to either BG or pepstatin A. We were able to measure the fluorescence lifetime of the BG and lysosome probes bound to their corresponding targets. In the case of the lysosome probes and SiR-SNAP, the lifetime did not change significantly compared to unbound probe. The SiR700-BG derivative showed a slight increase of lifetime. These data also support a mechanism in which fluorogenicity is based on a shift of the zwitterion-spirolactone equilibrium upon target binding.

We then investigated the performance of the new probes in live-cell microscopy. SiR700-actin and SiR700-tubulin proved to be cell-permeable and fluorogenic, as observed by confocal imaging (Figure 3). Imaging was possible directly after addition of the probes without additional washing steps (Supplementary Figure 4A,B, E,F). Confocal microscopy revealed that the photostability of SiR700-tubulin and SiR700-actin in live cells was comparable to the corresponding SiR-analogues which were previously shown to be highly photostable (Supplementary Figure 11).³ The SNAP-tag substrate SiR700-BG permitted labeling of live cells expressing a nuclear localized SNAP-tag (Supplementary Figure 4G). Application of either SiR700-lysosome or SiR-lysosome to human fibroblasts resulted in a dotted distribution of fluorescence in the cytosol, which is characteristic for lysosomes (Figure 3 and Supplementary Figure 4D,H). The high fluorogenicity of these two probes permitted imaging without any washing steps. We evaluated the specificity of SiR- and SiR700-lysosome by colocalizing them with CellLight Lysosomes-RFP, a highly selective genetically encoded lysosome marker (Lamp1-tagRFP fusion). The observed high Pearson coefficient confirmed the specificity of the two probes (Supplementary Figure 5).

We next investigated the possibility to perform dual-color live cell imaging experiments with carboxy-SiR650 and carboxy-SiR700. Analysis of the excitation and emission spectra of carboxy-SiR650 and carboxy-SiR700 suggested that they can be excited by a single line between 630–640 nm and distinguished through their emission spectra (Supplementary Figure 6A). Simultaneous acquisition also allows correcting for cross-talk between SiR650 and SiR700 by a simple image subtraction procedure (Supplementary Figure 6C). As an example of the utility of this fluorophore pair for dual color imaging, we

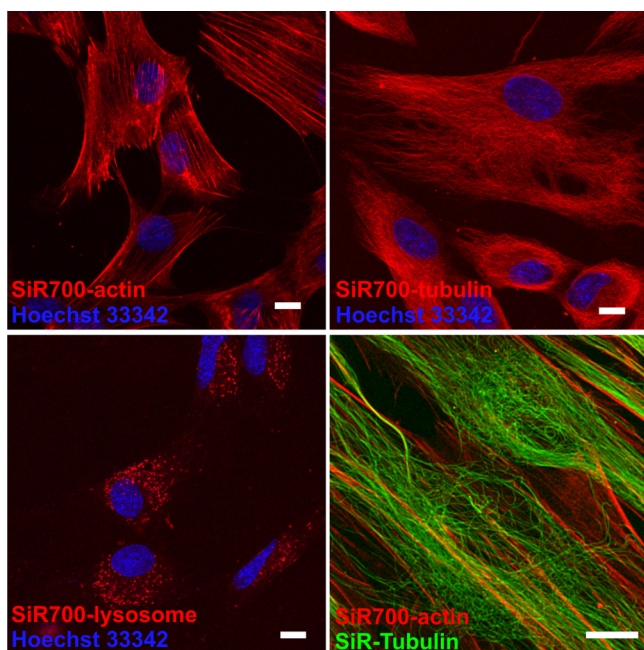


Figure 3. Confocal images of human primary fibroblasts stained with the corresponding probes. The SiR700-probe image is presented in red and overlaid with Hoechst 33342 nuclear staining in blue or SiR-tubulin in green. Cells were incubated with 2 μM probe for 1 h at 37 $^{\circ}\text{C}$ in growth medium. No washing was done before imaging. Scale bars = 10 μm .

imaged F-actin and microtubules in live human fibroblasts using SiR700-actin and SiR-tubulin (Figure 3). Next, we imaged lysosome movement along microtubules in live human primary fibroblasts using SiR700-tubulin and SiR-lysosome. Lysosomes move along microtubules at about 1 $\mu\text{m}/\text{s}$. Precise colocalization of such fast moving objects requires simultaneous acquisition. In addition to SiR700-tubulin and SiR-lysosome, we also included the nuclear stain Hoechst 33342 in these experiments. All three fluorophores can be imaged simultaneously using confocal microscopy, and we were able to image lysosome movements along microtubules with a >1 Hz frame rate (Supplementary Video 1). A noteworthy aspect of this experiment is that imaging of endogenous targets was possible through the simultaneous addition of three synthetic probes without any washing steps, which to our knowledge has not been previously reported and which underscores the power of fluorogenic probes.

The utility of any fluorescent probe is greatly enhanced when it is compatible with superresolution techniques. Therefore, we investigated the compatibility of SiR700 probes with structured illumination (SIM)¹⁵ and stimulated emission depletion (STED) microscopy.¹⁶ Microtubules are popular structures for benchmarking since their diameter of ~ 25 nm is well below the diffraction limit of conventional light microscopy. Using SiR700-tubulin in live primary human fibroblasts, we obtained ~ 140 and ~ 60 nm apparent microtubule diameter in SIM and STED images, respectively (Figure 4A, Supplementary Figure 7). The performance of SiR700-tubulin in both types of superresolution microscopy was comparable to that of SiR-tubulin measured with these set-ups (Supplementary Figure 7E). It should be noted that, while a 775 nm STED beam for inhibiting the fluorescence of carboxy-SiR700 yielded a good resolution enhancement, a STED beam of 800 nm wavelength is better suited, as it entails much reduced re-excitation. In

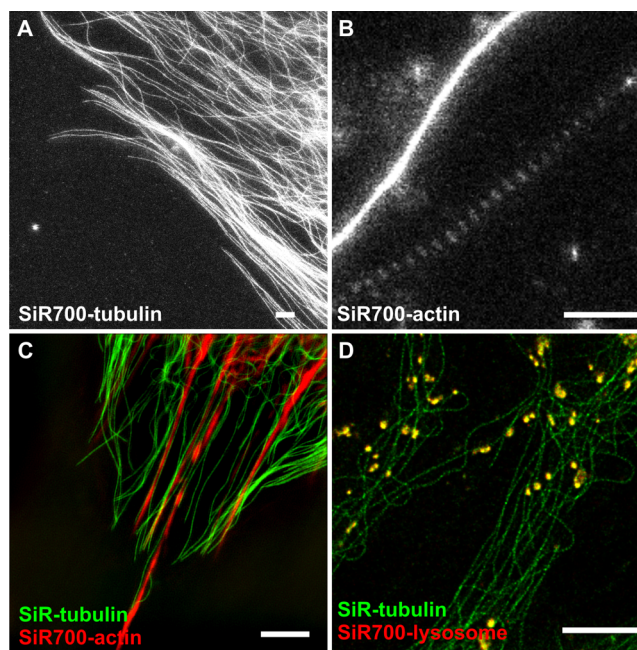


Figure 4. Superresolution microscopy with carboxy-SiR probes. (A) STED nanoscopy images of human primary fibroblasts stained with SiR700-tubulin probe for 1 h at 37 $^{\circ}\text{C}$. (B) STED images of primary rat hippocampal neurons stained with SiR700-actin probes for 1 h at 37 $^{\circ}\text{C}$. (C) Two-color SIM nanoscopy of human primary fibroblasts stained with SiR-tubulin (green) and SiR700-actin (red). (D) Two-color STED nanoscopy of living human primary fibroblasts stained with SiR-tubulin (green) and SiR700-lysosome (red). Scale bars = 1 μm (A,B) and 5 μm (C,D).

contrast, the optimal STED beam wavelength for carboxy-SiR650 is 775 nm.

Next, we evaluated the performance of SiR700-actin. We used SiR700-actin to image the periodical arrangement of actin cytoskeleton in the axon and dendrites of neurons, a striking and recent discovery.^{4,17,18} We previously reported periodic actin patterns in the axons of live neurons stained with SiR-actin. The spacing of the actin lattice measured in the axons of live neurons stained with SiR700-actin was ~ 190 nm, which coincides with what we measured previously with SiR-actin (Figure 4B, Supplementary Figure 8). The two new probes for lysosome imaging were also compatible with STED and SIM. When used in live-cell STED microscopy, SiR-lysosome yielded a higher resolution as compared to its confocal counterpart (Supplementary Figure 9).

Finally, we performed dual-color superresolution microscopy with our far-red probes based on carboxy-SiR650 and carboxy-SiR700. For live-cell SIM we modified a commercial NIKON N-SIM system by mounting an additional commercial filter cube optimized for the emission light of SiR700 into the turret. This simple upgrade allowed a selective detection of SiR650 and SiR700 excited by a single 640 nm laser. Using a single and standard 640 nm excitation line greatly simplifies the acquisition of SIM image with SiR700, as the interference pattern does not have to be calibrated for a new excitation wavelength. SIM images of live human primary fibroblasts stained with SiR700-actin and SiR-tubulin allowed the detection of F-actin and microtubules with minor cross-talk at sub-diffraction resolution (Figure 4C and Supplementary Figure 10A,C). We also performed live-cell, dual-color STED imaging experiments using SiR-tubulin together with SiR700-

lysosome or SiR-tubulin together with SiR700-actin. A commercial Leica TCS SP8 STED 3× microscope equipped with a 775 nm STED laser was used in these experiments. The resulting images display microtubules more sharply; the same holds for actin and lysosome structures (Figure 4D and Supplementary Figure 10B,D). These experiments demonstrate how SiR-based probes can be used for far-red, dual-color superresolution microscopy.

Our new probes based on carboxy-SiR700 for live-cell imaging of actin, microtubules, lysosomes, and SNAP-tag are fluorogenic, cell-permeable, and compatible with superresolution microscopy. They are well suited, in conjunction with our previously introduced carboxy-SiR650-based probes, for far-red, dual-color superresolution microscopy. Image recording after simple addition of the probes to the samples was possible without additional washing steps, highlighting the importance of fluorogenicity of synthetic probes for live-cell applications. Furthermore, the two SiR-based probes utilize a part of the wavelength spectra that permits simultaneous use with most genetically encoded fluorescent probes. This compatibility opens up exciting opportunities for multicolor imaging. As a result, SiR700-based probes greatly expand the potential of live-cell microscopy.

■ ASSOCIATED CONTENT

📄 Supporting Information

The Supporting Information is available free of charge on the ACS Publications website at DOI: 10.1021/jacs.6b04782.

Supplementary Video 1, showing lysosome movements along microtubules (AVI)

Supplementary figures, tables, and schemes; synthetic procedures; and characterizations of the compounds (PDF)

■ AUTHOR INFORMATION

Corresponding Authors

*grazvydas.lukinavicius@epfl.ch

*luc.reymond@epfl.ch

* kai.johnsson@epfl.ch

Author Contributions

#G.L. and L.R. contributed equally to the present work.

Notes

The authors declare the following competing financial interest(s): K.J., K.U., and G.L. have filed a patent application on SiR derivatives. L.R. and K.J. are cofounders of Spirochrome Ltd, Switzerland, which commercializes SiR derivatives.

■ ACKNOWLEDGMENTS

This work was supported by the Swiss National Science Foundation (K.J.), the NCCR Chemical Biology (K.J.), and the Lithuanian-Swiss cooperation program (K.J. and G.L., project CH-3-ŠMM-01/11). Technical assistance by Dr. Jana Doehner and Carmen Kaiser (University of Zürich), Elodie Cuenot (EPFL), and the Biomolecular Screening Facility of EPFL is acknowledged.

■ REFERENCES

- (1) Hell, S. W. *Angew. Chem., Int. Ed.* **2015**, *54*, 8054.
- (2) Lavis, L. D.; Raines, R. T. *ACS Chem. Biol.* **2014**, *9*, 855.
- (3) Lukinavicius, G.; Umezawa, K.; Olivier, N.; Honigsmann, A.; Yang, G.; Plass, T.; Mueller, V.; Reymond, L.; Correa, I. R., Jr.; Luo, Z.

G.; Schultz, C.; Lemke, E. A.; Heppenstall, P.; Eggeling, C.; Manley, S.; Johnsson, K. *Nat. Chem.* **2013**, *5*, 132.

(4) Lukinavicius, G.; Reymond, L.; D'Este, E.; Masharina, A.; Gottfert, F.; Ta, H.; Guthier, A.; Fournier, M.; Rizzo, S.; Waldmann, H.; Blaukopf, C.; Sommer, C.; Gerlich, D. W.; Arndt, H. D.; Hell, S. W.; Johnsson, K. *Nat. Methods* **2014**, *11*, 731.

(5) Lukinavicius, G.; Blaukopf, C.; Pershagen, E.; Schena, A.; Reymond, L.; Derivery, E.; Gonzalez-Gaitan, M.; D'Este, E.; Hell, S. W.; Wolfram Gerlich, D.; Johnsson, K. *Nat. Commun.* **2015**, *6*, 8497.

(6) Legant, W. R.; Shao, L.; Grimm, J. B.; Brown, T. A.; Milkie, D. E.; Avants, B. B.; Lavis, L. D.; Betzig, E. *Nat. Methods* **2016**, *13*, 359.

(7) Huang, Y.-L.; Walker, A. S.; Miller, E. W. *J. Am. Chem. Soc.* **2015**, *137*, 10767.

(8) Butkevich, A. N.; Mitronova, G. Y.; Sidenstein, S. C.; Klocke, J. L.; Kamin, D.; Meineke, D. N. H.; D'Este, E.; Kraemer, P.-T.; Danzl, J. G.; Belov, V. N.; Hell, S. W. *Angew. Chem., Int. Ed.* **2016**, *55*, 3290.

(9) Jack, T.; Simonin, J.; Ruepp, M.-D.; Thompson, A. J.; Gertsch, J.; Lochner, M. *Neuropharmacology* **2015**, *90*, 63.

(10) Erdmann, R. S.; Takakura, H.; Thompson, A. D.; Rivera-Molina, F.; Allgeyer, E. S.; Bewersdorf, J.; Toomre, D.; Schepartz, A. *Angew. Chem., Int. Ed.* **2014**, *53*, 10242.

(11) Uttamapinant, C.; Howe, J. D.; Lang, K.; Beránek, V.; Davis, L.; Mahesh, M.; Barry, N. P.; Chin, J. W. *J. Am. Chem. Soc.* **2015**, *137*, 4602.

(12) Koide, Y.; Urano, Y.; Hanaoka, K.; Piao, W.; Kusakabe, M.; Saito, N.; Terai, T.; Okabe, T.; Nagano, T. *J. Am. Chem. Soc.* **2012**, *134*, 5029.

(13) Please note that carboxy-SiR700-based probes are abbreviated as SiR700 probes, whereas probes based on carboxy-SiR650 are referred to simply as SiR probes.

(14) Chen, C. S.; Chen, W. N.; Zhou, M.; Arttamangkul, S.; Haugland, R. P. *J. Biochem. Biophys. Methods* **2000**, *42*, 137.

(15) Gustafsson, M. G. *J. Microsc.* **2000**, *198*, 82.

(16) Hell, S. W.; Wichmann, J. *Opt. Lett.* **1994**, *19*, 780.

(17) D'Este, E.; Kamin, D.; Gottfert, F.; El-Hady, A.; Hell, S. W. *Cell Rep.* **2015**, *10*, 1246.

(18) Xu, K.; Zhong, G.; Zhuang, X. *Science* **2013**, *339*, 452.